

Maximizing the geometric measure of entanglement

Jonathan Steinberg and Otfried Gühne

*Naturwissenschaftlich-Technische Fakultät, Universität Siegen, Walter-Flex-Straße 3, 57068 Siegen, Germany**

(Dated: October 26, 2022)

The characterization of the maximally achievable entanglement in a given physical system is relevant, as entanglement is known to be a resource for various quantum information tasks. This holds especially for pure multiparticle quantum states, where the problem of maximal entanglement is not only of physical interest, but also closely related to fundamental mathematical problems in multilinear algebra and tensor analysis. We propose an algorithmic method to find maximally entangled states of several particles in terms of the geometric measure of entanglement. Besides identifying physically interesting states our results deliver insights to the problem of absolutely maximally entangled states; moreover, our methods can be generalized to identify maximally entangled subspaces.

Introduction.— Quantum entanglement is central for applications like quantum metrology or quantum cryptography, where it allows to outperform classical resources [1–3]. Consequently, quantum states which exhibit a maximal amount of entanglement are candidates for resourceful states and for a given physical system, it is natural to ask for the maximal entanglement that can be contained in it. For the two-particle case, the maximally entangled states are the generalized Bell states. These serve as a unit of entanglement and so the identification of maximally entangled multiparticle states may contribute to the quest of determining minimal reversible entanglement generating sets [4–6].

Apart from its practical relevance, the problem is also from a purely theoretical point of view highly nontrivial. In multiparticle systems the phenomenon of entanglement monogamy expresses the fact that one party, say Alice, cannot be maximally entangled with Bob and, at the same time, be maximally entangled with Charlie [7]. This puts strong constraints on the possible entanglement distribution and stresses that multiparticle entanglement offers a complex structure. Indeed, the amount of entanglement present in a system cannot be captured by a single number [4]. This results in a variety of quantifiers, each emphasizing a different property that makes a state a valuable resource [8–10]. A prominent example is the notion of absolutely maximally entangled (AME) states which are notoriously difficult to characterize [11–16]. Still, the analysis of AME states is important for understanding quantum error correction and regarded as one of the central problems in the field [17, 18].

The geometric measure of entanglement [19–22], measuring the proximity of a quantum state to the set of product states, has an intuitive meaning and also offers multiple operational interpretations. For instance, it relates to multipartite state discrimination using LOCC [23], the additivity of channel capacities [24], quantum state estimation [25] and was also used to describe quantum phase transitions [26–29]. Further, it has been realized that generic quantum states are highly entangled [30]. In complexity theory, identifying max-

imally entangled states and computing their geometric measures allows for the identification of cases where the MAX- N -local Hamiltonian problem and its product state approximation deviate maximally [31, 32]. So, although high entanglement does not guarantee that a quantum state is useful for all tasks [33–35], finding maximally entangled states has been recognised as a natural and important problem [32]. So far, however, maximally entangled states have only been identified within the low-dimensional family of symmetric qubit states, where their computation is related to the problem of distributing charges on the unit sphere [10, 36], or within the family of graph states that stem from bipartite graphs [37].

Mathematically, the complexity of the task reflects the fact that pure multiparticle states are described by tensors. In contrast to the matrix case, notions like ranks and eigenvalues are for tensors much less understood and their computation turns out to be a hard problem [38, 39]. Interestingly, the geometric measure is closely related to the recently introduced concept of tensor eigenvalues [21, 40–43] as well as to the notion of injective tensor norms [44, 45] and matrix permanents [46]. Here, maximally entangled states offer maximal tensor eigenvalues [47] and it was conjectured that the overlap of a multipartite qubit state with the set of product states decreases exponentially in the number of particles [45]. So, the identification of maximally entangled states provides valuable intuition to decide this conjecture.

In this paper we design an iterative method for finding maximally entangled states with respect to geometric measure. Choosing initially a generic multiparticle quantum state, we show that in each step of the algorithm the geometric measure increases. We apply the algorithm to various multiparticle systems and identify for moderate sizes the corresponding states, revealing an interesting connection to AME states. Further, we demonstrate the flexibility of our method by applying it to the search of maximally entangled subspaces and provide a full characterization for the case of three qubits.

The geometric measure.— This measure quantifies how well a given multiparticle quantum state can be approx-

imated by pure states. More formally [19–22], given $|\varphi\rangle$ one defines $G(|\varphi\rangle) = 1 - \lambda^2(|\varphi\rangle)$ with

$$\lambda^2(|\varphi\rangle) = \max_{|\pi\rangle} |\langle\pi|\varphi\rangle|^2, \quad (1)$$

where the maximization runs over all product states $|\pi\rangle$ of the corresponding system. This quantity for pure states can be extended to mixed states via the convex roof construction and is then a proper entanglement monotone [21].

While computing λ^2 for general pure state is, in principle, difficult [48], there is a simple see-saw iteration that can be used [49–51]. For a three-partite state $|\varphi\rangle$, the algorithm starts with a random product state $|a_0 b_0 c_0\rangle$. From this we can compute the non-normalized state $|\tilde{a}\rangle = \langle b_0 c_0 | \varphi \rangle$, and make the update $|a_0\rangle \mapsto |a_1\rangle = |\tilde{a}\rangle / \sqrt{\langle \tilde{a} | \tilde{a} \rangle}$. The procedure is repeated for the second qubit $|b_0\rangle$, starting in the product state $|a_1 b_0 c_0\rangle$. This is then iterated until one reaches a fixed point. Of course, this fixed point is not guaranteed to be the global optimum, in practice, however, this method works very well.

Idea of the algorithm.— We present the algorithm for the case of three qubits. The generalization to arbitrary multiparticle systems is straightforward and is discussed in Appendix A [52]. As initial state $|\varphi\rangle$ we choose a random pure three qubit state. Then, we compute its closest product state $|\pi\rangle$ via the see-saw algorithm described above. We can assume without loss of generality that $|\pi\rangle = |000\rangle$. We write $\lambda = |\langle\varphi|\pi\rangle|$ for the maximal overlap of $|\varphi\rangle$ with the set of all product states. Note that for a generic quantum state the closest product state is unique.

The key idea is now to perturb the state $|\varphi\rangle$ in a way that the overlap with $|\pi\rangle$ decreases. If $|\pi\rangle$ is the unique closest product state and the perturbation is small, one can then expect that the overlap with *all* product states decreases. So, we consider the orthocomplement of $|\pi\rangle = |000\rangle$, that is, the complex subspace spanned by $|001\rangle, |010\rangle, |100\rangle, |011\rangle, |101\rangle, |110\rangle, |111\rangle$. This subspace gives rise to a projection operator $\Pi = \mathbb{1} - |\pi\rangle\langle\pi|$ and we compute the best approximation of the state $|\varphi\rangle$ within this subspace, given by $|\eta\rangle = \Pi|\varphi\rangle/\mathcal{M}$, where \mathcal{M} denotes the normalization. Then, we shift the state $|\varphi\rangle$ in the direction of $|\eta\rangle$ by some small amount $\theta > 0$. Hence the state update rule is given by

$$|\varphi\rangle \mapsto |\tilde{\varphi}\rangle := \frac{1}{\mathcal{N}}(|\varphi\rangle + \theta|\eta\rangle) \quad (2)$$

where \mathcal{N} is a normalization factor.

In the next step, we calculate the best rank one approximation to $|\tilde{\varphi}\rangle$. This process is iterated until the geometric measure is not increasing under the update rule (2). In this case, one can reduce the step size or the algorithm terminates.

One can directly check that the overlap with $|\pi\rangle$ is

smaller for $|\tilde{\varphi}\rangle$ than for $|\varphi\rangle$. Indeed one has

$$|\langle\pi|\tilde{\varphi}\rangle|^2 = \frac{1}{\mathcal{N}^2} |\langle\pi|\varphi\rangle + \theta\langle\pi|\eta\rangle|^2 = \frac{\lambda^2}{\mathcal{N}^2} < \lambda^2 \quad (3)$$

since $\mathcal{N} > 1$ if $\theta > 0$. In fact, a much stronger statement holds:

Observation 1. For a generic quantum state $|\psi\rangle$ there always exists a $\Theta > 0$ such that the updated state $|\tilde{\psi}\rangle$ according to Eq. (2) with step size $\theta < \Theta$ fulfills $G(|\tilde{\psi}\rangle) < G(|\psi\rangle)$.

The proof is given in Appendix A [52], so this observation can indeed be turned into an observer-independent fact. Observation 1 thus guarantees that the proposed algorithm yields a sequence of states with increasing geometric measure. Interestingly, the proof does not use the fact that $|\pi\rangle$ is a product state, so any figure of merit based on maximizing the overlap with pure states from some subset can be optimized with our method.

Implementation.— Thanks to the update rule in Eq. (2), we can make use of advanced descent optimization algorithms in order to obtain faster convergence and higher robustness against local optima [53, 54]. We have implemented a descent algorithm with momentum as well as the Nesterov accelerated gradient (NAG) [55]. The idea behind the momentum version is to keep track of the direction of the updates. More precisely, the update direction $|\eta_n\rangle$ in the n -th iteration will be a running average of the previously encountered updates $|\eta_1\rangle, \dots, |\eta_{n-1}\rangle$. For the NAG method, the update vector is, contrary to Eq. (2), evaluated at a point estimated from previous accumulated updates, and not at $|\varphi\rangle$. A more detailed discussion and a comparison of the different methods can be found in Appendix B [52]. The convergence of the algorithm in the case of qubits is also shown in Fig. 1.

After the algorithm has terminated, one obtains a tensor presented in a random basis. In order to identify the state and to obtain a concise form, we have to find appropriate local basis for each party, such that the state becomes as simple as possible. This can be done by a suitable local unitary transformation, see Appendix C for details [52].

Results for qubits.— For two qubits, the maximally entangled state is the Bell state and our algorithm directly converges to this maximum. For the case of three qubits there are two different equivalence classes of genuine tripartite entangled states with respect to stochastic local operations and classical communication (SLOCC) [56], namely $|W\rangle = (|001\rangle + |010\rangle + |100\rangle)/\sqrt{3}$ and $|GHZ\rangle = (|000\rangle + |111\rangle)/\sqrt{2}$. While $G(|GHZ\rangle) = 1/2$ one has $G(|W\rangle) = 5/9$, what turns out to be the maximizer among all tripartite states [6]. Indeed, after 150 iterations, the algorithm yields the W state. It should be noted, that in this case the maximizer belongs to the family of symmetric states. Operationally, the W state

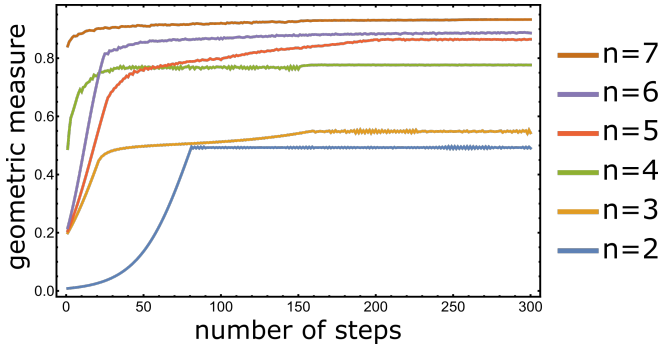


FIG. 1. Performance of the algorithm for multi-qubit systems. Initializing with a random state, for each iteration the geometric measure G is computed. The step size θ depends on the size of the system and we have $\theta_{n=2} = \theta_{n=3} = 0.01$ and $\theta_{n=6} = 0.06$. For the case $n = 3$, the slope starts to decrease when a measure of $G \approx 0.5$ is reached, coming from the fact that the GHZ state is an exceptional point of the function and yields $G(|\text{GHZ}\rangle) = 0.5$. A similar behaviour can be observed for $n = 4$ for the $|M\rangle$ and $|L\rangle$ state.

is the state with the maximal possible bipartite entanglement in the reduced two-qubit states [56].

For four qubits, the algorithm yields after 300 iterations the state

$$|\tilde{M}\rangle = \frac{1}{\sqrt{3}}(|\text{GHZ}\rangle + e^{2\pi i/3}|\text{GHZ}_{34}\rangle + e^{4\pi i/3}|\text{GHZ}_{24}\rangle) \quad (4)$$

where $|\text{GHZ}_{ij}\rangle$ means a four-qubit GHZ state where a bit flip is applied at party i and j . Note that the phases form a trine in the complex plane and that the state is a phased Dicke state [57]. This state can be shown to be LU-equivalent to the so called Higuchi-Sudbery or M state [14, 58], which appears as maximizer of the Tsallis α -entropy in the reduced two-particle states for $0 < \alpha < 2$. Note that this state is not symmetric with respect to permutations of the parties. Similar to the W state, the entanglement of the state in Eq. (4) appears to be robust, that is, uncontrolled decoherence of one qubit does not completely destroy the entanglement of the remaining qubits [58].

For five qubits the algorithm converges to a state $|G_5\rangle$, that can be identified with the ring cluster state (a 5-cycle graph state) yielding a geometric measure of $0.86855 \approx \frac{1}{36}(33 - \sqrt{3})$. The state $|G_5\rangle$ appears in the context of the five-qubit error correcting code [59]. Some basic facts concerning cluster and graph states are given in Appendix D [52]. Similarly, for six qubits we obtain a graph state $|G_6\rangle$ with a measure of $0.9166 \approx \frac{11}{12}$. This is again connected to quantum error correction, indeed, both states $|G_5\rangle$ and $|G_6\rangle$ are AME states, see also below. For seven qubits, we find a numerical state with maximally mixed two-body marginals, where the spectra of the three-body marginals are all the same. This motivates to introduce the class of maximally marginal

n	G_{\max}	$ \varphi\rangle_{\max}$
2	$\frac{1}{2}$	$ \psi^-\rangle$
3	$0.5555 \approx \frac{5}{9}$	$ W\rangle$
4	$0.7777 \approx \frac{7}{9}$	$ M\rangle$
5	$0.8686 \approx \frac{1}{36}(33 - \sqrt{3})$	$ G_5\rangle$
6	$0.9166 \approx \frac{11}{12}$	$ G_6\rangle$
7	≥ 0.941	MMS(7, 2)

TABLE I. Maximally entangled states found by the algorithm for systems between two and seven qubits. Here $|\varphi\rangle_{\max}$ refers to the state found by algorithm and G_{\max} denotes the geometric measure of corresponding state.

symmetric states (MMS), as a natural extension of notion of AME states.

Relation to AME states.— One calls a multiparticle state AME, if it is a maximally entangled state for any bipartition. For bipartite entanglement measures, it is well known that pure states with maximally mixed marginals are the maximally entangled states [58, 60, 61]. Consequently, an n -partite pure multi-qudit state is AME if all reductions to $\lfloor \frac{n}{2} \rfloor$ parties are maximally mixed, such a state is then denoted by $\text{AME}(n, d)$. Interestingly, not for all values of n and d AME states exist and quest for AME states is a central problem in entanglement theory [17]. The non-existence of AME states was first encountered for four qubits [58], but interestingly, the M state in Eq. (4) that maximizes the geometric measure can be viewed as the best possible replacement, since the one-body marginals are maximally mixed and all 2-body marginals, albeit not being maximally mixed have the same spectrum [14]. For five and six qubits the states found by our algorithm are just the known AME states, see also Appendix D [52]. For $n \geq 7$ no $\text{AME}(n, 2)$ state exist [11, 15]. A potential approximation $|F\rangle$ to the AME state of seven qubits has been identified [15], which is a graph state corresponding to the Fano plane. This state has a measure of $G(|F\rangle) = 15/16 = 0.9375$, thus smaller as the measure of the MMS state found by the algorithm.

While for certain values of n and d no AME state exists, it appears that multiple AME states can exist for other choices. In fact, it has been shown that those states can be even SLOCC inequivalent [62, 63]. It is in general a difficult problem to decide whether two states belong to the same SLOCC class, but for the case of AME states it can be drastically simplified using our algorithm in combination with the Kempf-Ness theorem [64]. First, notice that states with maximally mixed 1-body marginals belong to the so-called class of critical states [65]. The theorem then assures that two critical states belong to the same SLOCC class if and only if they are LU equivalent. Hence, if the geometric measure of those states differs, it already implies SLOCC inequivalence.

Systems of higher dimensions.— For the bipartite case the generalized Bell states $|\phi_d\rangle = \sum_{j=0}^{d-1} |jj\rangle / \sqrt{d}$ are max-

imally entangled with $G(|\phi_d\rangle) = 1 - 1/d$. We find that for $2 \leq d \leq 10$ the algorithm yields the corresponding state $|\psi_d\rangle$ with high fidelity, and that the number of iterations needed until convergence appears to be independent of d , see also Appendix B [52].

In the three-qutrit case we obtain the total antisymmetric state $|\Psi_3\rangle$, given by

$$|\Psi_3\rangle = \frac{1}{\sqrt{6}}(|012\rangle + |201\rangle + |120\rangle - |210\rangle - |102\rangle - |021\rangle) \quad (5)$$

In general, antisymmetric states $|\Psi_n\rangle$ can be constructed for all n -partite n -level systems and their geometric measure can be easily computed analytically as $\frac{n!-1}{n!}$ [66]. In the particular case $n = 3$ we obtain $G = \frac{5}{6} \approx 0.8333$. Note that $|\Psi_3\rangle$ is an AME state.

More generally, in the tripartite case a procedure is known to construct AME states for arbitrary d [67]. This leads to

$$\text{AME}(3, d) \sim \sum_{i,j=0}^{d-1} |i\rangle|j\rangle|i+j\rangle, \quad (6)$$

where $i+j$ is computed modulo d . Note that the state $\text{AME}(3, 3)$ constructed according to Eq. (6) only has a measure of $2/3$.

For the case of three ququads our algorithm gives insights into the AME problem. First, the $\text{AME}(3, 4)$ state corresponding to Eq. (6) has a geometric measure of $G = 0.75$. However, our algorithm yields a state given by

$$|\phi_{3,4}\rangle = \frac{1}{2\sqrt{2}}(|022\rangle + |033\rangle + |120\rangle + |131\rangle + |212\rangle + |203\rangle + |310\rangle + |301\rangle) \quad (7)$$

with $G(|\phi_{3,4}\rangle) = 7/8 = 0.875$. In addition, $|\phi_{3,4}\rangle$ is an AME state, i.e., all one-party marginals are maximally mixed. As the geometric measure of both states differs, they belong to different SLOCC classes. To our knowledge, the state $|\phi_{3,4}\rangle$ has not appeared in the literature before. Note that this is an AME state which is not of minimal nor maximal support [63, 68, 69].

In the case of four qutrits the algorithm converges to a state with a geometric measure of $0.888 \approx \frac{8}{9}$. This state can be identified to be the $\text{AME}(4, 3)$ state given by [67]

$$\begin{aligned} \text{AME}(4, 3) = \frac{1}{3}(&|0000\rangle + |0112\rangle + |0221\rangle + |1011\rangle + |1120\rangle \\ &+ |1202\rangle + |2022\rangle + |2101\rangle + |2210\rangle) \end{aligned} \quad (8)$$

For four ququads, the algorithm converges to the antisymmetric state $|\Psi_4\rangle$, yielding a measure of $\frac{23}{24} \approx 0.9583$. Interestingly, while being 1-uniform, this state is not AME. The so far only known $\text{AME}(4, 4)$, a graph state

[63, 70], yields a measure of $\frac{15}{16} = 0.9375$. Finally, the recently found $\text{AME}(4, 6)$ [18] is not maximally entangled with respect to the geometric measure, i.e., the algorithm finds states yielding a higher geometric measure.

Similarly, there exists a general procedure to construct $\text{AME}(5, d)$ states given by [67, 71]

$$\text{AME}(5, d) \sim \sum_{i,j,l=0}^{d-1} \omega^{il} |i\rangle|j\rangle|i+j\rangle|l+j\rangle|l\rangle, \quad (9)$$

where $\omega = e^{2\pi i/d}$. In the case of a three-dimensional system, the algorithm converges to the $\text{AME}(5, 3)$ state yielding a measure of approximately 0.96122. Finally, we have $G(\text{AME}(5, 4)) = \frac{31}{32} = 0.96875$. Here the algorithm yields a state $|\phi_{5,4}\rangle$ with a larger geometric measure, in particular $G(|\phi_{5,4}\rangle) > 0.975$. However, here we cannot identify a closed expression of the state. The numerical result suggests that the maximizer is again an AME state.

Maximally entangled subspaces.— One can extend our method such that it also applies to subspaces. More precisely, we want to construct an orthonormal basis for a subspace V such that the least entangled state in V is as entangled as possible in comparison with all other possible subspaces. Note that this notion differs from the concept of genuine entangled subspaces (GES) [72], where all states within the subspace have to be genuine entangled. However, our algorithm can readily be modified in order to search for GES with maximal genuine multipartite entanglement.

We will explain the idea of the algorithm for a two-dimensional subspace of three qubits. First, we choose a two-dimensional subspace randomly, which can be described by a projector of the form $P = |v\rangle\langle v| + |w\rangle\langle w|$, where $\langle v|w\rangle = 0$. Next, we compute the best rank-one approximation to P given by taking the argmax of $\sup_{abc} \text{Tr}[|abc\rangle\langle abc|P]$. This can be done with the iteration described after Eq. (1). Again we call the optimizer $|\pi\rangle$. More generally, the optimization yields the best product state approximation to the state in the range of P that is least entangled. In particular, this implies that if $\text{im}(P)$ contains a product state, the assigned geometric measure will be zero. Then we compute the eigenvectors corresponding to the two largest eigenvalues of the operator $P - \theta|\pi\rangle\langle\pi|$ that we will call $|v_1\rangle$ and $|v_2\rangle$. Clearly, this algorithm reduces to the one from the previous sections, if we choose the rank of the projector to be one.

It is known [73], that the maximal dimension of a subspace of an n -partite qudit system which contains no product state is given by $\dim(V) = d^n - dn + n - 1$. Consequently, for two qubits, the maximal entangled subspace is of dimension one and spanned by a Bell state. Indeed, if we apply our algorithm to larger subspaces, the measure we assign to this subspaces stays zero.

For three qubits, the algorithm converges to the W

state as one basis vector and to the state

$$|V\rangle = \frac{1}{\sqrt{3}}[|011\rangle + e^{\frac{2\pi}{3}i}|110\rangle + e^{\frac{4\pi}{3}i}|101\rangle] \quad (10)$$

as the other. The subspace spanned by $|W\rangle$ and $|V\rangle$ then has a remarkable property: all states are maximally entangled, yielding the same geometric measure as the W state. This has potential applications in information processing: In this subspace, qubit states may be encoded and then any set of these states is difficult to discriminate by local means [23].

Concerning higher dimensions, we computed the maximally entangled subspace of dimension two for two qutrits. Here we obtain an embedded Bell state $|\chi_1\rangle = (|01\rangle - |10\rangle)/\sqrt{2}$ and the state

$$|\chi_2\rangle = \frac{1}{\sqrt{14}}[|20\rangle + |02\rangle + \sqrt{6}(|21\rangle + |12\rangle)] \quad (11)$$

which can also be seen as the superposition of two Bell pairs. It turns out that the least entangled state within this subspace has a geometric measure of $1/2$. Again, applications can be envisaged, as any state in this subspace has at least one ebit of entanglement.

Conclusion— In this work we have presented a method for the computation of maximally entangled quantum states with respect to the geometric measure. We provided a convergence analysis and showed that in each step the entanglement of the iterates increase. The application of this algorithm allowed us to identify interesting

quantum states, discover novel AME states, and characterize highly entangled subspaces which may be useful for information processing.

Concerning further research, the introduced method may be used to find new AME states for cases where the existence is still open, e.g., for systems consisting of more than five quhex, or to find new SLOCC inequivalent AME states. From a mathematical perspective, the algorithm can give insights into the structure of tensor spaces and could offer intuition to solve open problems concerning the asymptotics of tensor norms [45]. Finally, the algorithm may be rephrased to apply to other quantifiers of quantumness, like coherence [74], and can be then used to study these resources in quantum information science.

We thank Guillaume Aubrun, Mariami Gachechiladze, Felix Huber, H. Chau Nguyen, René Schwonek, Liqun Qi, Franz Josef Stoiber, Nikolai Wyderka, Guofeng Zhang, and Karol Życzkowski for inspiring discussions. The University of Siegen is kindly acknowledged for enabling our computations through the OMNI cluster. This work was supported by the Deutsche Forschungsgemeinschaft (DFG, German Research Foundation, project numbers 447948357 and 440958198), the Sino-German Center for Research Promotion (Project M-0294), the ERC (Consolidator Grant 683107/TempoQ) and the German Ministry of Education and Research (Project QuKuK, BMBF Grant No. 16KIS1618K). JS acknowledges support from the House of Young Talents of the University of Siegen.

Appendix A: Proof of Observation 1

Let us first recapitulate the algorithm and fix the notation. Let $|\psi\rangle$ be the randomly drawn initial state and denote by $|\pi\rangle$ its best product state approximation (BPA), that is,

$$|\pi\rangle = \operatorname{argmin}\{|\pi\rangle : 1 - |\langle\varphi|\pi\rangle|^2 : |\pi\rangle \text{ product state}\}. \quad (12)$$

In particular, we can choose $|\pi\rangle$ such that $\lambda := \langle\pi|\psi\rangle > 0$. This allows for the computation of the update direction, $|\eta\rangle := (\Pi|\psi\rangle)/\mathcal{M}$, where $\Pi := \mathbb{1} - |\pi\rangle\langle\pi|$ is the projector onto the orthocomplement of the span of the BPA $|\pi\rangle$ and \mathcal{M} a normalization such that $\langle\eta|\eta\rangle = 1$. It follows directly that $\mathcal{M}^2 = \langle\psi|P|\psi\rangle = 1 - \lambda^2$, hence $\mathcal{M} = \sqrt{1 - \lambda^2}$. For a fixed step size $\theta > 0$, the update rule is given by

$$|\psi\rangle \mapsto |\tilde{\psi}\rangle := \frac{1}{\mathcal{N}}(|\psi\rangle + \theta|\eta\rangle). \quad (13)$$

where \mathcal{N} is again a normalization. In the following, we will frequently make statements about generic states. In these cases, we require the assumptions that a state is not a product state and that the BPA $|\pi\rangle$ is unique up to a phase.

The first step in order to prove monotonicity of the algorithm is to show that small variations in the initial state can only lead to small variations in the BPA. As we will see, this follows from the more general observation that under certain conditions the value y_0 , where a function $f(x_0, y)$ assumes its minimum (for a given x_0), depends continuously on x_0 . Further, by virtue of the canonical embedding, we can identify any $|\varphi\rangle \in \mathbb{C}^n$ with a $|\tilde{\varphi}\rangle \in \mathbb{R}^{2n}$ and consequently we can omit the absolute in Eq. (12). Then we have:

Lemma 1. Let X, Y be compact and $f : X \times Y \rightarrow \mathbb{R}$ be uniformly continuous. Further, suppose that for $x_0 \in X$ the value $y_0 := \operatorname{argmin}_{y \in Y} f(x_0, y)$ is unique. Then for all $\varepsilon > 0$ there exists $\delta > 0$ such that for all $x \in U_\delta(x_0)$ we have $\operatorname{argmin}_{y \in Y} f(x, y) \subset U_\varepsilon(y_0)$, where $U_\delta(x_0)$ and $U_\varepsilon(y_0)$ denote vicinities of x_0 and y_0 , respectively. In other words, the function argmin is continuous in x_0 .

Proof. For the given ε we can split the set Y in the vicinity $U_\varepsilon(y_0)$ and its complement $\overline{U}_\varepsilon(y_0)$. In particular we have

$$\begin{aligned} f(x_0, y_0) &= \min_{y \in U_\varepsilon(y_0)} f(x_0, y) \\ &< \min_{y \in \overline{U}_\varepsilon(y_0)} f(x_0, y) =: f(x_0, \tilde{y}_0), \end{aligned} \quad (14)$$

that is, \tilde{y}_0 denotes the value where the minimum in $\overline{U}_\varepsilon(y_0)$ is assumed. Let us denote the difference between the function values as

$$\xi = f(x_0, \tilde{y}_0) - f(x_0, y_0) > 0. \quad (15)$$

By the uniform continuity we can choose $\delta > 0$ such that for all $\tilde{x} \in \mathbb{R}^n$ with $\|\tilde{x} - x_0\| < \delta$ and for all y we have

$$|f(\tilde{x}, y) - f(x_0, y)| < \frac{\xi}{2}. \quad (16)$$

Then we have

$$f(\tilde{x}, y_0) < f(x_0, y_0) + \frac{\xi}{2}, \quad (17)$$

but for all $y \in \overline{U}_\varepsilon(y_0)$

$$f(\tilde{x}, y) > f(x_0, \tilde{y}_0) - \frac{\xi}{2} > f(x_0, y_0) + \frac{\xi}{2}, \quad (18)$$

which implies that the minimum of $f(\tilde{x}, y)$ lies in the vicinity $U_\varepsilon(y_0)$. \square

Corollary 2. Let $|\varphi\rangle$ be a pure quantum state and suppose that its BPA $|\pi\rangle$ is unique. Then, for all $\tau > 0$, there exists a $\xi > 0$ such that the BPA $|\tilde{\pi}\rangle$ of $|\tilde{\varphi}\rangle \in \mathcal{U}_\xi(|\varphi\rangle)$ lies in $\mathcal{U}_\tau(|\pi\rangle)$.

Proof. The function $f(x, y) := |\langle x, y \rangle|^2$ is continuous on $\mathbb{R}^{2n} \times \mathbb{R}^{2n}$. Further, the space $B_1 := \{x \in \mathbb{R}^{2n} : \|x\| = 1\}$ is compact and thus also $M := B_1 \times B_1$. Then, by the Heine-Cantor theorem [75], f is uniformly continuous on M . Since we assume $|\pi\rangle$ to be unique, we can apply Lemma 1, which guarantees for all $\tau > 0$ the existence of $\xi > 0$ such that $|\tilde{\pi}\rangle \in U_\tau(|\pi\rangle)$ for $|\tilde{\psi}\rangle \in U_\xi(|\psi\rangle)$. \square

According to Eq. (13), the updated state needs a renormalization given by $\mathcal{N} = \mathcal{N}(|\psi\rangle, \theta)$. The next ingredient for the proof of the main result is a Lemma that gives later an upper approximation of the function $1/\mathcal{N}$.

Lemma 3. There exists $C > 0$ such that for all $q \in [0, 1]$ and $x > 0$ we have

$$\frac{1}{\sqrt{1 + 2qx + x^2}} < 1 - qx + Cx^2. \quad (19)$$

More precisely, the above inequality holds for all $C \geq 3$.

Proof. As both sides of Eq. (19) are positive, we can square them such that the inequality remains true. This yields the equivalent inequality

$$\begin{aligned} 0 &< [2C - 3q^2 + 1]x^2 + 2q[C - 1 + q^2]x^3 + [C^2 - C(4q^2 - 2) + q^2]x^4 + 2q[C^2 - C]x^5 + C^2x^6 \\ &=: f_2x^2 + f_3x^3 + f_4x^4 + f_5x^5 + f_6x^6 \end{aligned} \quad (20)$$

Now observe that for each of the constants $f_k = f_k(C)$ there is a $C_k > 0$ such that $f_k(C) \geq 0$ for all $C \geq C_k$. Indeed, we have $C_2 := \max\{(1/2)(3q^2 - 1), 0\}$, $C_3 := 1 - q^2$, $C_5 = C_6 := 1$. The choice of C_4 depends on whether $q^2 \geq 1/2$ or not. If we denote $\alpha = |4q^2 - 2|$, we obtain for the case $q^2 < 1/2$ that $C^2 + \alpha C + q^2 > 0$, what is trivially fulfilled for any $C \geq 1$. If $q^2 > 1/2$, we need $C^2 - \alpha C + q^2 > 0$. But $C^2 - \alpha C + q^2 \geq C^2 - \alpha C = C(C - \alpha) > 0$, we obtain $C > \alpha$. In general, we have $C_4 := \max\{1, |4q^2 - 2|\}$. This implies that for $C \geq \tilde{C} := \max\{C_k \mid k = 2, \dots, 6\}$ all coefficients are positive. Hence $0 < f_2x^2$ implies $0 < f_2x^2 + f_3x^3 + f_4x^4 + f_5x^5 + f_6x^6$ if $x > 0$. Consequently, it is sufficient to only consider the problem $0 < f_2x^2$, what is true for $C \geq C_7 := (1/2)(3q^2 - 1)$. Hence, choosing $C \geq \max\{\tilde{C}, C_7\}$ yields the claim. Taking the maximum over all C_k with respect to $q \in [0, 1]$ yields that $C > 2$. \square

Theorem 4. Let $|\psi\rangle$ be a generic pure quantum state. Then there exists $\Theta > 0$ such that for the updated state $|\tilde{\psi}\rangle$ according to Eq. (2) with step-size $\Theta > \theta > 0$ we have $G(|\psi\rangle) < G(|\tilde{\psi}\rangle)$.

Proof. Let us start with some step-size $\theta_0 > 0$ that we will choose in the end appropriately and consider

$$|\tilde{\psi}\rangle = \frac{1}{\mathcal{N}}(|\psi\rangle + \theta_0|\eta\rangle). \quad (21)$$

It is important to note that $|\eta\rangle$ is a normalized state, that is, $|\eta\rangle = 1/(\sqrt{1-\lambda^2})(\mathbb{1} - |\pi\rangle\langle\pi|)|\psi\rangle$. This yields $\langle\psi|\eta\rangle = \sqrt{1-\lambda^2}$.

The BPA $|\tilde{\pi}\rangle$ of $|\tilde{\psi}\rangle$ can be parameterized using the old product state, i.e., $|\tilde{\pi}\rangle = \sqrt{1-\delta^2}|\pi\rangle + \delta|\chi\rangle$, for a normalized, appropriately chosen $|\chi\rangle$ and $\delta > 0$. Using $\langle\pi|\eta\rangle = 0$ and $|\langle\chi|\eta\rangle| \leq 1$ we obtain

$$\tilde{\lambda} := |\langle\tilde{\pi}|\tilde{\psi}\rangle| = \frac{1}{\mathcal{N}}|\langle\tilde{\pi}|\psi\rangle + \theta_0\delta\langle\chi|\eta\rangle| \leq \frac{1}{\mathcal{N}}(|\langle\tilde{\pi}|\psi\rangle| + |\theta_0\delta\langle\chi|\eta\rangle|) \leq \frac{1}{\mathcal{N}}(\lambda + \delta\theta_0). \quad (22)$$

Using that $\mathcal{N} = \sqrt{1 + 2\theta_0\sqrt{1-\lambda^2} + \theta_0^2}$ and Lemma 3 there exists $C > 0$ such that

$$\begin{aligned} \tilde{\lambda} &< (1 - \theta_0\sqrt{1-\lambda^2} + C\theta_0^2)(\lambda + \delta\theta_0) \\ &= \lambda + \delta\theta_0 - \lambda\sqrt{1-\lambda^2}\theta_0 + \theta_0^2[C(\lambda + \delta\theta_0) - \delta\sqrt{1-\lambda^2}] \\ &= \lambda + \theta_0(\delta - \lambda\sqrt{1-\lambda^2}) + \mathcal{O}(\theta_0^2). \end{aligned} \quad (23)$$

Note that $\lambda\sqrt{1-\lambda^2} > 0$, since $0 \neq \lambda \neq 1$. This comes from the fact that a generic state is not a product state with $\lambda = 1$ and any state has at least some overlap with some product state. So, if $\delta < \lambda\sqrt{1-\lambda^2}$ we have $\tilde{\lambda} < \lambda$ for suitably small θ_0 .

It remains to show that we can guarantee that δ obeys this condition. We start with a given value of λ and consider a number $0 < \delta_1 < \lambda\sqrt{1-\lambda^2}$. According to Corollary 2, we can find a $\theta_1 > 0$ such that $|\tilde{\pi}\rangle \in U_{\delta_1}(|\pi\rangle)$ if $|\tilde{\psi}\rangle \in U_{\theta_1}(|\psi\rangle)$. Then, this gives us an upper bound on θ_0 for Eq. (21), so that the resulting $\delta < \delta_1$ in Eq. (23) is small enough to guarantee a negative slope for the linear term. Still, $\tilde{\lambda} < \lambda$ is not guaranteed, due to the $\mathcal{O}(\theta_0^2)$ term in Eq. (23). But, for the given values of λ, δ_1 and C , we can also compute from Eq. (23) a second threshold θ_2 , which guarantees $\tilde{\lambda} < \lambda$. Then we can take finally in the statement of the Theorem $\Theta = \min\{\theta_1, \theta_2\}$ and the proof is complete. \square

It is remarkable that in this proof the fact that $|\pi\rangle$ is a product state was never used. So, the algorithm can also be used if the overlap with states from some other subset of the (pure) state space shall be minimized.

Appendix B: Performance of the algorithm

In the following we explain our choice of the step-size θ , the number of iterations and the duration of the computation. First, it should be noticed that the algorithm contains the computation of the closest product state as a subroutine. Because the see-saw is prone to local maxima, we randomize the algorithm, i.e., we run the iteration for many different initial states. The number of iterations as well as the number of initial states depends on the number of parties and the local dimension. The iteration typically converges fast, e.g. for three qubits 10 iterations are sufficient and for five ququads 30 iterations. The number of initial states can for small systems be chosen small, e.g., for three qubits 10 different initial points make the largest overlap robust while for larger systems more initial states are necessary, e.g., for five ququads 100 points were taken.

The step-size θ used in the update rule Eq. (13) depends on the size of the system and on the variation of the measure of the iterates. For systems of small and moderate size, we initially choose $\theta = 0.01$. After a certain number of iterations (mostly around 400) the measure of the iterates is not increasing anymore, but fluctuates around a certain value where the amount of fluctuation depends on the step-size. In this case the step-size is reduced via $\theta = \theta/2$ and one proceeds with the new step-size. However, if θ becomes small it is also useful to improve the precision in the computation of the best product state approximation.

Because the update rule resembles the idea of a gradient descent (GD), we can make use of advanced gradient descent techniques as the momentum method (CM) [76] or Nesterov's accelerated gradient (NAG) [55]. In the general setting one aims to minimize a (typically complicated and high-dimensional) real-valued function $f(\omega)$. Suppose that one initializes the parameters to ω_0 . In the GD, the parameters are iteratively updated according to $\omega_{t+1} = \omega_t - \kappa_t$,

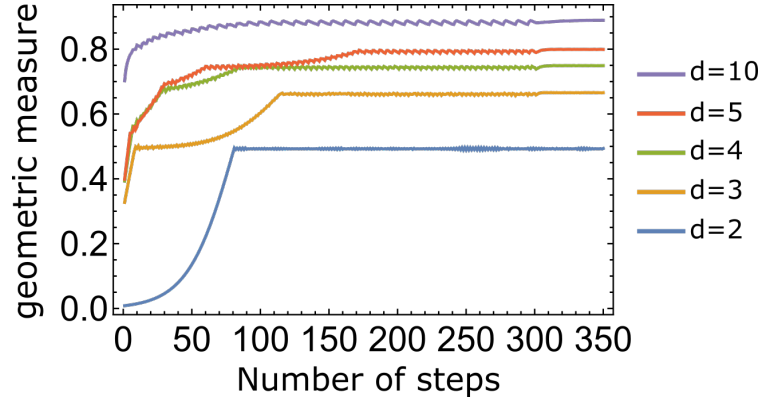


FIG. 2. Convergence of the algorithm for bipartite systems of different local dimension $d \in \{2, 3, 4, 5, 10\}$. For local dimension $d \leq 5$ we have chosen the step-size as $\theta = 0.01$. For $d = 10$ the step-size was chosen as $\theta = 0.1$. After 350 iterations, the iterates had a very high fidelity with the qudit Bell state.

where $\kappa_t = \theta_t(\nabla_{\omega} f)(\omega_t)$ with step-size $\theta_t > 0$, and $(\nabla_{\omega} f)(\omega_t)$ is the gradient of f evaluated at ω_t . The idea behind CM is to keep track about the direction we are moving in parameter space. For a given momentum parameter $\gamma \in [0, 1]$ the update is given by $\kappa_t = \gamma\kappa_{t-1} + \theta_t(\nabla_{\omega} f)(\omega_t)$. Clearly, κ_t is a running average of previously calculated gradients. The advantage of using CM is that the momentum enhances the decrease in directions with small gradients while suppressing oscillations in high-curvature directions.

For NAG, the idea is to not calculate the gradient with respect to the current parameter ω_t , that is $(\nabla_{\omega} f)(\omega_t)$, but at the expected value of the parameters given the recent momentum, that is, $(\nabla_{\omega} f)(\omega_t) + \gamma\kappa_{t-1}$. Accordingly, the NAG update rule is given by $\omega_{t+1} = \omega_t - \kappa_t$ where $\kappa_t = \gamma\kappa_{t-1} + \theta_t(\nabla_{\omega} f)(\omega_t + \gamma\kappa_{t-1})$.

The update rule in Eq. (13) naturally invites for two different variants. First, as introduced in the main text, the update direction $|\eta\rangle = (1/\sqrt{\langle\psi|\Pi|\psi\rangle})\Pi|\psi\rangle$ can be re-normalized. This has the consequence that the amount of the shift stays constant for all iterations. However, a second option would be to take just the projected (un-normalized) state $\Pi|\psi\rangle$ as the update. Here, the size of the shift changes within each iteration, depending on how large the state $|\psi\rangle$ is supported within the subspace $\text{im}(\Pi)$.

Appendix C: Unitary optimization

After a sufficient number of iterations, the algorithm yields a state given by coordinates with respect to a random basis. Hence, generically each component of the tensor is nonzero. However, in order to understand the structure of the state, we seek for a concise representation in which most of the coefficients vanish. As we consider two states to be equal if there is a LU-transformation connecting them, this requires a parametrization of the set of unitary matrices. First notice, that $U(d)$ is the semidirect product of $U(1)$ with $SU(d)$ and hence we can restrict to parametrizations of $SU(n)$. For qubits, one can make use of the fact that $SU(2)$ is diffeomorphic to the 3-sphere S^3 . In particular, an arbitrary $SU(2)$ matrix can be written as

$$U = \begin{pmatrix} \alpha & -\beta^* \\ \beta & \alpha^* \end{pmatrix}, \quad \alpha, \beta \in \mathbb{C} \text{ with } |\alpha|^2 + |\beta|^2 = 1 \quad (24)$$

Consequently, the parametrization involves four real parameters and one quadratic constraint. However, for $d \geq 3$ the $SU(d)$ is not even homeomorphic to a sphere, or a product of them, e.g., $SU(3)$ is *not* homeomorphic to S^8 . Consequently, for systems of higher dimensions different approaches exist [77–79]. In our work, we have used the Jarlskog parametrization [78], what is a simple recursive scheme for parametrization, which can be easily implemented numerically. First, notice that any $X \in U(d)$ can be written as $X = \Phi_{\alpha} Y \Phi_{\beta}$ where $\Phi_{\alpha} = \text{diag}(e^{i\alpha_1}, \dots, e^{i\alpha_n})$, Φ_{β} similar and Y a unitary $n \times n$ matrix. Now, Y is decomposed into a product of unitaries, that is, $Y = \prod_{k=2}^d A_{d,k}$ with

$$A_{d,k} = \begin{pmatrix} A^{(k)} & 0 \\ 0 & \mathbb{1}_{d-k} \end{pmatrix}, \quad U(d) \ni A^{(k)} = \begin{pmatrix} \mathbb{1}_{d-1} - (1 - \cos(\theta_k))|a_k\rangle\langle a_k| & \sin(\theta_k)|a_k\rangle \\ -\sin(\theta_k)\langle a_k| & \cos(\theta_k) \end{pmatrix}, \quad (25)$$

where $|a_k\rangle \in \mathbb{C}^{d-1}$ normalized to one, i.e., $\langle a_k|a_k\rangle = 1$ and $\theta_k \in [0, 2\pi)$ an arbitrary angle.

We now describe how this parametrization can be used to bring the numerically found states into a concise form. Here, two different cases can be considered. If one has a guess for the possible state, e.g., the marginals are all maximally mixed so one expects an AME state, one could compute the fidelity between the numerical state $|\psi\rangle$ and the guess $|\varphi_{\text{guess}}\rangle$, i.e., $\sup|\langle\psi|U_1 \otimes \dots \otimes U_n|\varphi_{\text{guess}}\rangle|$. If there is no possible candidate, the idea is to minimize a function $f: \text{U}(d) \times \dots \times \text{U}(d) \rightarrow \mathbb{R}$ depending on the state, which becomes minimal if many entries of the state vanish. For instance, given the state $|\psi\rangle$ a natural candidate would be $f(U_1, \dots, U_n) = \sum |(U_1 \otimes \dots \otimes U_n|\psi\rangle)_{i_1, \dots, i_n}|$. Given two states $|\phi\rangle, |\psi\rangle$ we regard them as equal, if $\mathcal{F}(|\psi\rangle, |\phi\rangle) \geq 1 - \epsilon$ with $\epsilon < 10^{-6}$, where \mathcal{F} denotes the fidelity.

Appendix D: Known AME graph states and their graphs

In this section we present the graphs of the corresponding graph states mentioned in the main text and explain their construction. There are two equivalent methods how a graph state could be defined, namely via a quantum circuit in terms of a sequence of commuting unitary two-qubit operations or alternatively using the stabilizer formalism [80]. Here we use the first approach. A graph $G = (V, E)$ is a set of $|V|$ vertices and some edges $E \subset V \times V$ connecting them. A graph state $|G\rangle$ associated to a graph G is a pure quantum state on $(\mathbb{C}^2)^{\otimes |V|}$ built up of Ising type interactions according to

$$|G\rangle = \prod_{(a,b) \in E} \text{CZ}_{a,b} |+\rangle^{\otimes |V|} \quad \text{where} \quad \text{CZ}_{a,b} = \sum_{k=0}^1 |k\rangle\langle k|_a \otimes Z_b^k \quad (26)$$

where Z_b denotes σ_z only acting on system b and similar for $\mathbb{1}_a$. The AME(4,4) state can be built up out of 8 qubits, that are grouped together as $A = \{1, 2\}, B = \{3, 4\}, C = \{5, 6\}, D = \{7, 8\}$, while the Ising type interaction is implemented as described in Eq. (26).

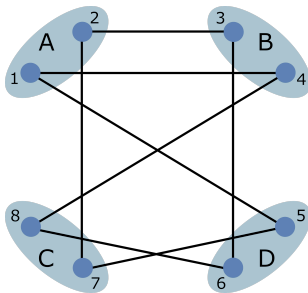


FIG. 3. Graph of the known AME(4,4) state [70].

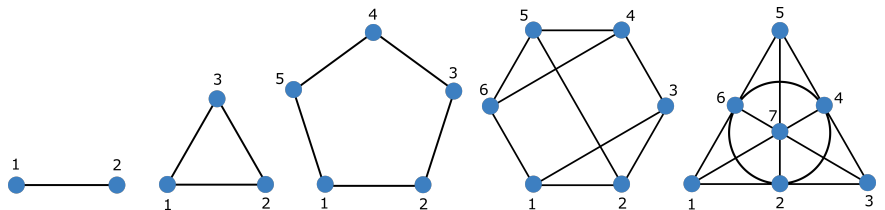


FIG. 4. Highly entangled qubit graph states. The first four graphs yielding the known AME states on two/three/five/six qubits respectively. The last graph state, the Fano graph state [15], is a 2-uniform state on seven qubits where 32 of its 35 three-body marginals are maximally mixed.

* steinberg@physik.uni-siegen.de

- [1] C. H. Bennett and G. Brassard, “Quantum cryptography: Public key distribution and coin tossing,” *Theor. Comput. Sci.* **560**, 7–11 (2014).
- [2] A. K. Ekert, “Quantum cryptography based on Bell’s theorem,” *Phys. Rev. Lett.* **67**, 661 (1991).
- [3] M. J. Holland and K. Burnett, “Interferometric detection of optical phase shifts at the Heisenberg limit,” *Phys. Rev. Lett.* **71**, 1355 (1993).
- [4] C. H. Bennett, S. Popescu, J. A. Smolin, and A. V. Thapliyal, “Exact and asymptotic measures of multipartite pure-state entanglement,” *Phys. Rev. A* **63**, 012307 (2000).
- [5] J. Eisert, P. Hyllus, O. Gühne, and M. Curty, “Complete hierarchies of efficient approximations to problems in entanglement theory,” *Phys. Rev. A* **70**, 062317 (2004).

- [6] S. Tamaryan, T. C. Wei, and D. Park, “Maximally entangled three-qubit states via geometric measure of entanglement,” *Phys. Rev. A* **80**, 052315 (2009).
- [7] V. Coffman, J. Kundu, and W. K. Wootters, “Distributed entanglement,” *Phys. Rev. A* **61**, 052306 (2000).
- [8] V. Vedral and M. B. Plenio, “Entanglement measures and purification procedures,” *Phys. Rev. A* **57**, 1619 (1998).
- [9] G. Vidal and R. Tarrach, “Robustness of entanglement,” *Phys. Rev. A* **59**, 141 (1998).
- [10] O. Giraud, P. Braun, and D. Braun, “Quantifying quantumness and the quest for queens of quantum,” *New J. Phys.* **12**, 063005 (2010).
- [11] A. J. Scott, “Multipartite entanglement, quantum-error-correcting codes, and entangling power of quantum evolutions,” *Phys. Rev. A* **69**, 052330 (2004).
- [12] P. Facchi, G. Florio, G. Parisi, and S. Pascazio, “Maximally multipartite entangled states,” *Phys. Rev. A* **77**, 060304(R) (2008).

- [13] R. Reuvers, “An algorithm to explore entanglement in small systems,” *Proc. R. Soc. A* **474** (2018), 10.1098/rspa.2018.0023.
- [14] G. Gour and N. R. Wallach, “All maximally entangled four-qubit states,” *J. Math. Phys.* **51**, 112201 (2010).
- [15] F. Huber, O. Gühne, and J. Siewert, “Absolutely maximally entangled states of seven qubits do not exist,” *Phys. Rev. Lett.* **118**, 200502 (2017).
- [16] F. Huber, C. Eltschka, J. Siewert, and O. Gühne, “Bounds on absolutely maximally entangled states from shadow inequalities, and the quantum MacWilliams identity,” *J. Phys. A* **51**, 175301 (2018).
- [17] P. Horodecki, L. Rudnicki, and K. Życzkowski, “Five open problems in quantum information theory,” *PRX Quantum* **3**, 010101 (2022).
- [18] S. A. Rather, A. Burchardt, W. Bruzda, G. Rajchel-Mieldzioc, A. Lakshminarayan, and K. Życzkowski, “Thirty-six entangled officers of Euler,” *Phys. Rev. Lett.* **128**, 080507 (2022).
- [19] A. Shimony, “Degree of entanglement,” *Ann. N. Y. Acad. Sci.* **755**, 675–679 (1995).
- [20] H. Barnum and N. Linden, “Monotones and invariants for multi-particle quantum states,” *J. Phys. A* **34**, 6787 (2001).
- [21] T.-C. Wei and P. M. Goldbart, “Geometric measure of entanglement and applications to bipartite and multipartite quantum states,” *Phys. Rev. A* **68**, 042307 (2003).
- [22] P. Badziąg, Č. Brukner, W. Laskowski, T. Paterek, and M. Żukowski, “Experimentally friendly geometrical criteria for entanglement,” *Phys. Rev. Lett.* **100**, 140403 (2008).
- [23] M. Hayashi, D. Markham, M. Murao, M. Owari, and S. Virmani, “Bounds on multipartite entangled orthogonal state discrimination using local operations and classical communication,” *Phys. Rev. Lett.* **96**, 040501 (2006).
- [24] A. Sen(De) and U. Sen, “Channel capacities versus entanglement measures in multiparty quantum states,” *Phys. Rev. A* **81**, 012308 (2010).
- [25] L. Chen, H. Zhu, and T.-C. Wei, “Connections of geometric measure of entanglement of pure symmetric states to quantum state estimation,” *Phys. Rev. A* **83**, 012305 (2011).
- [26] R. Orús and T. C. Wei, “Visualizing elusive phase transitions with geometric entanglement,” *Phys. Rev. B* **82**, 155120 (2010).
- [27] O. Buerschaper, A. García-Saez, R. Orús, and T.-C. Wei, “Topological minimally entangled states via geometric measure,” *J. Stat. Mech.*, 11009 (2014).
- [28] Q.-Q. Shi, H.-L. Wang, S.-H. Li, S. Y. Cho, M. T. Batchelor, and H.-Q. Zhou, “Geometric entanglement and quantum phase transitions in two-dimensional quantum lattice models,” *Phys. Rev. A* **93**, 062341 (2016).
- [29] A. Deger and T. C. Wei, “Geometric entanglement and quantum phase transition in generalized cluster-xy models,” *Quantum Inf. Process.* **18**, 326 (2019).
- [30] P. Hayden, D. W. Leung, and A. Winter, “Aspects of generic entanglement,” *Commun. Math. Phys.* **265**, 95–117 (2009).
- [31] S. Gharibian and J. Kempe, “Approximation algorithms for QMA-complete problems,” *SIAM J. Comput.* **41**, 1028–1050 (2012).
- [32] A. Montanaro, “Injective tensor norms and open problems in quantum information,” <https://people.maths.bris.ac.uk/~csxam/presentations/injnormtalk.pdf> (2012).
- [33] M. van den Nest, W. Dür, A. Miyake, and H. J. Briegel, “Fundamentals of universality in one-way quantum computation,” *New J. Phys.* **9**, 1–51 (2007).
- [34] M. J. Bremner, C. Mora, and A. Winter, “Are random pure states useful for quantum computation?” *Phys. Rev. Lett.* **102**, 190502 (2009).
- [35] D. Gross, S. T. Flammia, and J. Eisert, “Most quantum states are too entangled to be useful as computational resources,” *Phys. Rev. Lett.* **102**, 190501 (2009).
- [36] M. Aulbach, D. Markham, and M. Murao, “The maximally entangled symmetric state in terms of the geometric measure,” *New J. Phys.* **12**, 073025 (2010).
- [37] M. Hajdušek, and M. Murao, “Direct evaluation of pure graph state entanglement,” *New J. Phys.* **15**, 013039 (2013).
- [38] E. Chitambar, R. Duan, and Y. Shi, “Tripartite entanglement transformations and tensor rank,” *Phys. Rev. Lett.* **101**, 140502 (2008).
- [39] C. J. Hillar and L. H. Lim, “Most tensor problems are NP-hard,” *J. ACM* **60**, 1–39 (2013).
- [40] L. Qi, “Eigenvalues of a real supersymmetric tensor,” *J. Symb. Comput.* **40**, 1302–1324 (2005).
- [41] L. Chen, A. Xu, and H. Zhu, “Computation of the geometric measure of entanglement for pure multiqubit states,” *Phys. Rev. A* **82**, 032301 (2010).
- [42] G. Ni, L. Qi, and M. Bai, “Geometric measure of entanglement and U-eigenvalues of tensors,” *SIAM J. Matrix Anal. Appl.* **35**, 73–87 (2014).
- [43] S. Hu, L. Qi, and G. Zhang, “Computing the geometric measure of entanglement of multipartite pure states by means of non-negative tensors,” *Phys. Rev. A* **93**, 012304 (2016).
- [44] R. F. Werner and A. S. Holevo, “Counterexample to an additivity conjecture for output purity of quantum channels,” *J. Math. Phys.* **43**, 4353 (2002).
- [45] G. Aubrun and S. J. Szarek, “Alice and Bob Meet Banach: The Interface of Asymptotic Geometric Analysis and Quantum Information Theory,” (American Mathematical Society, 2017) Chap. 8.
- [46] T.-C. Wei and S. Severini, “Matrix permanent and quantum entanglement of permutation invariant states,” *J. Math. Phys.* **51**, 092203 (2010).
- [47] L. Qi, H. Chen, and Y. Chen, *Tensor Eigenvalues and Their Applications* (Springer Singapore, 2018).
- [48] V. de Silva and L.-H. Lim, “Tensor rank and the ill-posedness of the best low-rank approximation problem,” *SIAM J. Matrix Anal. Appl.* **30**, 1084–1127 (2008).
- [49] O. Gühne, M. Reimpell, and R. F. Werner, “Estimating entanglement measures in experiments,” *Phys. Rev. Lett.* **98**, 110502 (2007).
- [50] A. Streltsov, H. Kampermann, and D. Bruss, “Simple algorithm for computing the geometric measure of entanglement,” *Phys. Rev. A* **84**, 022323 (2011).
- [51] S. Gerke, W. Vogel, and J. Sperling, “Numerical construction of multipartite entanglement witnesses,” *Phys. Rev. X* **8**, 031047 (2018).
- [52] Supplemental Material, which includes the proof of Observation 1 and a discussion about optimization over the unitary group as well as the additional references [75–80].
- [53] Y. Nesterov, “Lectures on convex optimization,” (Springer, 2018) Chap. Nonlinear Optimization.

- [54] P. Mehta, M. Bukov, C.-H. Wang, A.G.R. Day, C. Richardson, C.K. Fisher, and D.J. Schwab, “A high-bias, low-variance introduction to machine learning for physicists,” *Phys. Rep.* **810**, 1–124 (2019).
- [55] Y. Nesterov, “A method for unconstrained convex minimization problem with the rate of convergence $o(1/k^2)$,” *Soviet. Math. Docl.* **269**, 543–547 (1983).
- [56] W. Dür, G. Vidal, and J. I. Cirac, “Three qubits can be entangled in two inequivalent ways,” *Phys. Rev. A* **62**, 062314 (2000).
- [57] P. Krammer, H. Kampermann, D. Bruß, R. A. Bertlmann, L. C. Kwek, and C. Macchiavello, “Multipartite entanglement detection via structure factors,” *Phys. Rev. Lett.* **103**, 100502 (2009).
- [58] A. Higuchi and A. Sudbery, “How entangled can two couples get?” *Phys. Lett. A* **273**, 213–217 (2000).
- [59] E. Knill, R. Laflamme, R. Martinez, and C. Negrevergne, “Benchmarking quantum computers: The five-qubit error correcting code,” *Phys. Rev. Lett.* **86**, 5811 (2001).
- [60] N. Gisin and H. Bechmann-Pasquinucci, “Bell inequality, Bell states and maximally entangled states for n qubits,” *Phys. Lett. A* **246**, 1–6 (1998).
- [61] G. Vidal, “Entanglement monotones,” *J. Mod. Opt.* **47**, 355–376 (2000).
- [62] Z. Raissi, A. Teixedó, C. Gogolin, and A. Acín, “Constructions of k -uniform and absolutely maximally entangled states beyond maximum distance codes,” *Phys. Rev. Research* **2**, 033411 (2020).
- [63] A. Burchardt and Z. Raissi, “Stochastic local operations with classical communication of absolutely maximally entangled states,” *Phys. Rev. A* **102**, 022413 (2020).
- [64] G. Kempf and L. Ness, “Algebraic geometry,” (Springer, Berlin, Germany, 1979) Chap. The length of vectors in representation spaces, pp. 233–243.
- [65] G. Gour and N. R. Wallach, “Necessary and sufficient conditions for local manipulation of multipartite pure quantum states,” *New J. Phys.* **13**, 073013 (2011).
- [66] M. Hayashi, D. Markham, M. Murao, M. Owari, and S. Virmani, “Entanglement of multiparty-stabilizer, symmetric, and antisymmetric states,” *Phys. Rev. A* **77**, 012104 (2008).
- [67] D. Goyeneche, Z. Raissi, S. Di Martino, and K. Życzkowski, “Entanglement and quantum combinatorial designs,” *Phys. Rev. A* **97**, 062326 (2018).
- [68] D. Goyeneche, D. Alsina, J. I. Latorre, A. Riera, and K. Życzkowski, “Absolutely maximally entangled states, combinatorial designs, and multiunitary matrices,” *Phys. Rev. A* **92**, 032316 (2015).
- [69] Z. Raissi, C. Gogolin, A. Riera, and A. Acín, “Optimal quantum error correcting codes from absolutely maximally entangled states,” *J. Phys. A* **51**, 075301 (2018).
- [70] W. Helwig, “Absolutely maximally entangled qudit graph states,” *arXiv*, 1306.287 (2013).
- [71] E. M. Rains, “Nonbinary quantum codes,” *IEEE Trans. Inf. Theory* **45**, 1827 (1999).
- [72] M. Demianowicz and R. Augusiak, “From unextendible product bases to genuinely entangled subspaces,” *Phys. Rev. A* **98**, 012313 (2018).
- [73] K. R. Parthasarathy, “On the maximal dimension of a completely entangled subspace for finite level quantum systems,” *Proc. Math. Sci.* **114**, 365–374 (2004).
- [74] T. Baumgratz, M. Cramer, and M. B. Plenio, “Quantifying coherence,” *Phys. Rev. Lett.* **113**, 140401 (2014).
- [75] G. K. Pedersen, “Analysis now,” (Springer New York, 1989) Chap. Hilbert Spaces, pp. 79–125.
- [76] B. T. Polyak, “Some methods for speeding up the convergence of iteration methods,” *USSR Comput. Math. and Math. Phys.* **4**, 1–17 (1964).
- [77] T. Tilma and E. C. G. Sudarshan, “Generalized Euler angle parametrization for $SU(n)$,” *J. Math. Phys.* **35**, 10467 (2002).
- [78] C. Jarlskog, “A recursive parametrization of unitary matrices,” *J. Math. Phys.* **46**, 103508 (2005).
- [79] C. Spengler, M. Huber, and B. C. Hiesmayr, “A composite parameterization of unitary groups, density matrices and subspaces,” *J. Phys. A* **43**, 385306 (2010).
- [80] M. Hein, J. Eisert, and H. J. Briegel, “Multiparty entanglement in graph states,” *Phys. Rev. A* **69**, 062311 (2004).